ISSN 0036-0236, Russian Journal of Inorganic Chemistry, 2008, Vol. 53, No. 5, pp. 800–804. © Pleiades Publishing, Ltd., 2008.
Original Russian Text © N.M. Kozhevnikova, T.N. Khamaganova, 2008, published in Zhurnal Neorganicheskoi Khimii, 2008, Vol. 53, No. 5, pp. 864–865.

PHYSICOCHEMICAL ANALYSIS OF INORGANIC SYSTEMS

NASICON Phases of Variable Composition $K_{1-x}A_{1-x}R_{1+x}(MoO_4)_3$ ($0 \le x \le 0.2–0.6$), where A = Ni, Mg, Co, or Mn and R = Yb, Lu, or Sc

N. M. Kozhevnikova and T. N. Khamaganova

Baikal Institute of Nature Management, Siberian Branch, Russian Academy of Sciences
ul. Sakh'anova 8, Ulan-Ude, Buryat Republic, 67004 Russia

Received March 1, 2007

Abstract—Phases of variable composition $K_{1-x}A_{1-x}R_{1+x}(MoO_4)_3$ ($0 \le x \le 0.2–0.6$), where A = Ni, Mg, Co, or Mn and R = Yb, Lu, or Sc, which crystallize in a NASICON-type structure (space group $R\bar{3}c$) were synthesized by solid-phase reactions. Their crystal parameters were calculated, and IR and Raman spectra described.

DOI: 10.1134/S0036023608050215

Structural analogues of NASICON are known among complex oxides in sulfate, phosphate, arsenate, and molybdate systems [1]. The considerable interest in the preparation and characterization of NASICON phases is due to their nonlinear optical, ferroelectric, and superionic properties and high thermal stability. Laser and luminescent materials have been prepared on the basis of these phases. The base of the crystal structure of the representatives of this family is a rhombohedral framework $\{[M_2(XO_4)_3]^{p-}\}_{3\infty}$, which is built of corner-sharing MO_6 octahedra and XO_4 tetrahedra. Low-charge alkali cations reside in interstices, which are connected into a system of channels with large and variable cross sections. This endows some NASICON phases, namely those having partially vacant alkali cation positions, with superionic conductivity [2].

NASICON structures have the following characteristic features: a high isomorphic capacity for extraframework cations and the possibility of isomorphic substitutions in the octahedra and tetrahedra of the framework. NASICON phases have a potential for use as solid electrolytes, catalysts, and matrices for immobilization of long-lived isotopes and toxins.

In a study of M_2MoO_4–$AMoO_4$–$R_2(MoO_4)_3$ systems where M = Na or K; A = Mg, Mn, Co, or Ni; and R = Al, Cr, or Fe, we synthesized triple molybdates $MAR(MoO_4)_3$ and phases of variable composition $M_{1-x}A_{1-x}R_{1+x}(MoO_4)_3$ ($0 \le x \le 0.3–0.5$), which are $MAR(MoO_4)_3$-based subtraction solid solutions [2]. The possibility of varying the cationic composition within one structure type offers a means for the targeted synthesis of NASICON phases; the necessary conditions for the appearance of this structure are the size of octahedral cations equal to 0.6–0.9 Å (R = Yb, Lu, or Sc; and A = Mg, Mn, Co, or Ni meet this condition) and the size of the extraframework cation K^+.

One goal in this work is to study the possibility of Yb, Lu, Sc, Mg, Mn, Co, and Ni octahedral cations entering the NASICON structure. Another goal is to determine the crystallization regions for triple molybdates $KAR(MoO_4)_3$ and their atom-vacancy solid solutions $K_{1-x}A_{1-x}R_{1+x}(MoO_4)_3$. Still another goal is to study crystal characteristics and discuss the effect of cation substitutions on the distortion of coordination polyhedra and cation distributions in some phases of variable composition.

EXPERIMENTAL

Interactions in systems K_2MoO_4–$AMoO_4$–$R_2(MoO_4)_3$ was studied in the subsolidus region at 450–800°C.

The starting components (K_2MoO_4, $NiMoO_4$, $MgMoO_4$, $CoMoO_4$, $MnMoO_4$, $Yb_2(MoO_4)_3$, $Lu_2(MoO_4)_3$, and $Sc_2(MoO_4)_3$) were presynthesized by ceramic technology from K_2CO_3, di- and tervalent metal oxides, and MoO_3. The study was carried out in two stages. First, the phase composition of the samples whose chemical composition corresponded to the meeting points of all sections in systems K_2MoO_4–$AMoO_4$–$R_2(MoO_4)_3$ was studied by X-ray diffraction. As a result, the system was triangulated. Second, the quasi-binary joins determined at the first stage were studied.

Triple molybdates $KAR(MoO_4)_3$ were found to form along sections $KR(MoO_4)_2$–$AMoO_4$ and $K_2A_2(MoO_4)_3$–$R_2(MoO_4)_3$ at 600–650°C (figure). Phases of variable composition $K_{1-x}A_{1-x}R_{1+x}(MoO_4)_3$ are formed in the plane of the triangle K_2MoO_4–$AMoO_4$–$R_2(MoO_4)_3$ and along the section $KAR(MoO_4)_3$–$R_2(MoO_4)_3$. Samples with compositions lying along quasi-binary joins were prepared in 25–5 mol % steps; for refining the composition of the triple molybdate $KAR(MoO_4)_3$ and the homogeneity regions of the phases of variable composition $K_{1-x}A_{1-x}R_{1+x}(MoO_4)_3$, the steps were 1 mol %. Samples were annealed at 450, 550, 600, 650, and 700°C. Nickel and cobalt samples were in addition annealed at 750 and 800°C with intermediate grinding every 20–30 h. The annealing time at each temperature was 80–100 h. Once annealed, samples were slowly cooled with the furnace. Nonequilibrated samples were annealed additionally. Equilibrium was considered acquired if the phase composition of a sample remained unchanged after two sequential anneals. Synthesis products were identified by X-ray powder diffraction (FR-552 monochromator camera, CuK_α radiation, Ge internal standard). Powder patterns were digitized on an IZA-2 comparator. The standard program package Rentgen was used to process X-ray diffraction patterns (Table 1).

Vibration spectra were recorded from polycrystalline $M_{1-x}A_{1-x}R_{1+x}(MoO_4)_3$ samples (Bruker FT-IR and Specord M80 spectrometers, excitation with near-IR laser (1.06 nm), reflection geometry, 3–5 cm^{-1} resolution). Test samples were Nujol mulls on polyethylene substrates or KBr disks. Molybdenum-isotope-substituted samples were prepared from $^{92}MoO_3$ and $^{100}MoO_3$. Vibration frequencies are compiled in Tables 2 and 3.

Differential thermal analysis (DTA) was performed on an MOM OD-103 derivatograph (temperature elevation rate, 10 K/min; sample sizes, 0.3–0.4 g).

RESULTS AND DISCUSSION

The interactions in systems K_2MoO_4–$AMoO_4$–$R_2(MoO_4)_3$ at 600–650°C are slow and do not go to completion. The annealing temperature was progressively elevated to 700–800°C. Annealing at 750–800°C for 150–200 h yielded single-phase $K_{1-x}A_{1-x}R_{1+x}(MoO_4)_3$ samples, whose homogeneity ranges de-pended on the two- and three-charged cations. Scandium phases with A = Mg or Mn have the greatest extent: $0 \le x \le 0.6$. For R = Yb or Lu and A = Mg or Mn, $0 \le x \le 0.3$. Phases $K_{1-x}Co(Ni)_{1-x}R_{1+x}(MoO_4)_3$ were obtained for R = Sc with $0 \le x \le 0.3$ and for R = Yb or Lu with $0 \le x \le 0.2$. Single-phase $K_{1-x}Co(Ni)_{1-x}R_{1+x}(MoO_4)_3$ samples were prepared at 800°C after 180–200 h of annealing. The figure illustrates phase relations in the system K_2MoO_4–$MgMoO_4$–$Sc_2(MoO_4)_3$; in the other systems, they are alike.

X-ray diffraction showed that the compounds $K_{1-x}A_{1-x}R_{1+x}(MoO_4)_3$ are isostructural to each other and the compound $Na_{0.625}Zn_{0.625}Sc_{1.375}(MoO_4)_3$ [3]; they crystallize in trigonal space group $R\bar{3}c$, $Z = 6$.

The structural base of compounds $K_{1-x}A_{1-x}R_{1+x}(MoO_4)_3$ is the framework assembly of octahedra $A(R)O_6$ and tetrahedra MoO_4. This structure is an analogue of corundum: atoms A(R) reside on three-fold axis, and MoO_4 groups on twofold axes. Vacant octahedral and tetrahedral voids merge into a three-dimensional system of channels, which are filled by potassium cations.

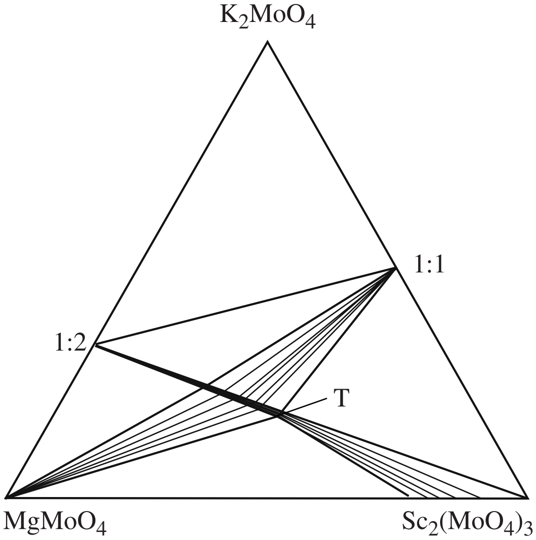

Phase relations in the system K_2MoO_4–$MgMoO_4$–$Sc_2(MoO_4)_3$ at 750°C. Notation: T = $K_{1-x}Mg_{1-x}Sc_{1+x}(MoO_4)_3$ $(0 \le x \le 0.6)$.

As x increases, the octahedral positions in the $K_{1-x}A_{1-x}R_{1+x}(MoO_4)_3$ structure, which are randomly occupied by di- and tervalent atoms, acquire an excess of the tervalent element and a deficit of the divalent one. Potassium, which resides in interstices, is also in a deficit. This cation distribution increases the contribution of R–O to the overall electrostatic balance of the structure. In order for the balance to be conserved, K–O bonds should weaken, which is provided by the deficit of extraframework potassium atoms and the increase in the framework size; the unit cell volume increases with increasing the $K_{1-x}A_{1-x}R_{1+x}(MoO_4)_3$ extent (Table 1).

The phases of variable composition $K_{1-x}A_{1-x}R_{1+x}(MoO_4)_3$ contain isolated distorted anionic tetrahedral groups MoO_4^{2-}, in their structure; therefore, we can comparatively analyze the internal vibrations in these groups and the external vibrations of cationic sublattices and tetrahedra MoO_4 as a whole. The bands associated with the vibrations of groups MoO_4^{2-} can experience an isotopic shift upon ^{92}Mo–^{100}Mo substitutions (Tables 2, 3).

X-ray crystallography shows that molybdenum atoms lay on twofold axes ($c2$) and atoms A and R on threefold axes ($c3$). The potassium site symmetry is $c3i$. The comparatively low symmetry of tetrahedra MoO_4 implies that degeneracy is released from their doubly and triply degenerate vibrations and that the components of the full-symmetry stretching vibrations are active in IR spectra.

Table 1. Crystal and thermal parameters for $K_{1-x}A_{1-x}R_{1+x}(MoO_4)_3$

Composition			*a*, Å	*c*, Å	*V*/*Z*, Å^3	T_m, °C
A	R	*x*				
Ni	Sc	0	9.422(2)	24.145(2)	309.4	1170
Ni	Sc	0.3	9.437(3)	24.153(5)	310.5	–
Ni	Lu	0	9.428(1)	24.437(5)	313.5	1150
Ni	Lu	0.2	9.439(4)	24.441(2)	314.3	–
Ni	Yb	0	9.430(2)	24.439(3)	313.6	1130
Ni	Yb	0.2	9.441(3)	24.445(1)	314.4	–
Mg	Sc	0	9.421(2)	24.414(5)	312.8	1100
Mg	Sc	0.3	9.440(6)	24.453(3)	314.5	–
Mg	Sc	0.6	9.451(2)	24.488(7)	315.7	–
Mg	Lu	0	9.491(1)	24.262(4)	315.5	1055
Mg	Lu	0.3	9.498(2)	24.285(3)	316.3	–
Mg	Yb	0	9.505(4)	24.312(6)	317.1	1030
Mg	Yb	0.3	9.512(2)	24.346(1)	317.9	–
Co	Sc	0	9.530(2)	24.345(5)	319.2	1120
Co	Sc	0.3	9.542(4)	24.354(2)	320.1	–
Co	Lu	0	9.557(2)	24.361(1)	321.1	1090
Co	Lu	0.2	9.586(3)	24.373(2)	323.3	–
Co	Yb	0	9.594(4)	24.382(3)	323.9	1070
Co	Yb	0.2	9.601(2)	24.399(5)	324.6	–
Mn	Sc	0	9.608(3)	24.417(6)	325.3	1060
Mn	Sc	0.3	9.611(1)	24.435(5)	325.8	–
Mn	Sc	0.6	9.627(4)	24.452(1)	327.1	–
Mn	Lu	0	9.634(5)	24.462(2)	327.7	1005
Mn	Lu	0.3	9.641(4)	24.485(3)	328.5	–
Mn	Yb	0	9.674(1)	24.503(4)	330.9	990
Mn	Yb	0.3	9.692(5)	24.526(3)	332.5	–

The group theory analysis implies the following distribution over irreducible representations for the factor group of space group $D3d$:

$$\Gamma_k = A_{1u}(\text{inact.}) + A_{2u}(\text{IR}) + E_u(\text{IR}),$$

$$\Gamma_{A+R} = A_{1g} + A_{2g}(\text{inact.}) + 2E_g(\text{Raman}) + A_{1u}(\text{inact.}) + A_{2u}(\text{IR}) + 2E_u(\text{IR}),$$

$$\Gamma_{Mo} = 3A_{2g}(\text{inact.}) + 3E_g(\text{Raman}) + 3A_{2u}(\text{IR}) + 3E_u(\text{IR}).$$

Three lines of the vibrations of cations A^{2+} and R^{3+} should be observed in the Raman spectrum; in the IR spectrum, there are two bands due to cations K^+ and three due to $A^{2+} + R^{3+}$. Six lines associated with the vibrations of MoO_4 groups should be observed in the Raman spectrum and nines bands in the IR spectrum.

The bands with frequencies of 980–760 cm^{-1} (stretching vibrations) and 410–300 cm^{-1} (bending vibrations) were assigned to the internal vibrations in

Table 2. Raman vibration frequencies, cm^{-1}

$KMnLu(MoO_4)_3$	$KMnLu(^{92}MoO_4)_3$	$KMnLu(^{100}MoO_4)_3$	$KMgLu(MoO_4)_3$	$K_{0.7}Mg_{0.7}Lu_{1.3}(MoO_4)_3$	$KCo Yb(MoO_4)_3$	$K_{0.8}Co_{0.8}Y_{1.2}(MoO_4)_3$	$KMgSc(MoO_4)_3$	$K_{0.7}Mg_{0.7}Sc_{1.3}(MoO_4)_3$	$K_{0.7}Mg_{0.7}Sc_{1.3}(MoO_4)_3$	Assignment
946	948	945	954	957	952	956	960	962	965	Stretching vibrations of MoO_4 groups
867	869	864	870	872	865	870	872	874	877	
828	830	826	830	828	826	828	827	829	832	
812	813	810	810	812	808	810	810	812	814	
			372	372	368	371	370	370	372	
348	348	348	350	352	348	350	350	350	352	
335	338	336	338	340	337	339	336	338	340	Bending vibrations of MoO_4 groups
272	272	270			272	272	261	261	261	Joint vibrations of M cations
			212	212			212	212	214	
196	196	196			197	197				
180	180	180			182	182	190	190	185	Vibrations of A^{2+} cations and translation vibrations of various sublattices
158	158	158			160	160	158	158	155	
140	140	140			140	140				
							124	124	123	
							82	82	84	

groups MoO_4; these bands, as a rule, experience shifts upon isotope substitution and lie in the spectral region characteristic of the vibrations in molybdenum–oxygen tetrahedra [4].

Three components correspond to the degenerate vibration in agreement with the low anion symmetry. The full-symmetry stretching vibrations of molybdate groups, which are distributed over two sets of crystallographic positions, are degenerate, probably because of the similar geometry and dynamics of these polyhedra. The stretching frequencies along the series $K_{1-x}A_{1-x}R_{1+x}(MoO_4)_3$ are less strongly affected by the nature of the cation but increase considerably with rising x (Tables 2, 3). This is likely due to the Mo–O bond energy increasing because of generation of extra cationic vacancies.

The vibrations of potassium cations are inactive in the Raman spectrum; the lines below 300 cm^{-1} are assigned to the vibrations of two- and three-charged cations, experience a shift upon cation substitutions Mn ⟶ Co ⟶ Mg and Yb ⟶ Lu ⟶ Sc, and are sensitive to molybdenum isotope substitutions (282–277 cm^{-1}). Bands in the IR spectra behave in a similar manner. The band at 190 cm^{-1} is due to the dominant vibration of scandium cations. The low-frequency Raman bands at 124–82 cm^{-1} experience a shift upon

Table 3. IR vibration frequencies, cm^{-1}

$KMnLu(MoO_4)_3$	$KMnLu(^{92}MoO_4)_3$	$KMnLu(^{100}MoO_4)_3$	$KMgLu(MoO_4)_3$	$K_{0.7}Mg_{0.7}Lu_{1.3}(MoO_4)_3$	$KCoYb(MoO_4)_3$	$K_{0.8}Co_{0.8}Yb_{1.2}(MoO_4)_3$	$KMgSc(MoO_4)_3$	$K_{0.7}Mg_{0.7}Sc_{1.3}(MoO_4)_3$	$K_{0.4}Mg_{0.4}Sc_{1.6}(MoO_4)_3$	Assignment
952	954	950	955	957	954	958	965	974	980	Stretching vibrations of MoO_4 groups
883	885	881	885	890	887	880	878	875	877	
835	833	836	837	837	835	838	833	834	836	
812	810	811	813	813	810	812	800	805	820	
408	403	405	412	407	405	403	412	407	407	Bending vibrations of MoO_4 groups
350	352	352	358	356	360	362	365	360	362	
305	305	305	309	309	309	308	312	312	312	
280	282	279	279	280	282	282	277	277	277	Joint vibrations of M cations
222	224	224	228	229	230	232				
213	213	213	213	213	215	215				
							190	190	190	Vibrations of A^{2+} and R^{3+} cations
147	150	150	152	152	154	156	158	158	158	
138	138	138	140	140	142	142	145	145	145	Vibrations of cations K^+ and librations of MoO_4 groups
109	109	109	114	114	118	118	123	123	123	

substitution Mn ⟶ Co ⟶ Mg and are assigned to the vibrations of A^{2+}. In the IR spectra, the bands below 160 cm^{-1} are assigned to the vibrations of potassium cations; the bands associated with the librations of molybdate groups appear in the same region [4].

The above-described study implies that excess three-charged cations are accommodated at A^{2+} sites upon aliovalent substitution $K + A^{2+} \longrightarrow R^{3+} + \square$, whereas the newly generated vacancies are located in the potassium sublattice.

REFERENCES

1. V. B. Kalinin, Izv. Akad. Nauk SSSR, Neorg. Mater. **26** (11), 2229 (1990).
2. N. M. Kozhevnikova and M. V. Mokhosoev, *Triple Molybdates* (Buryat State Univ., Ulan-Ude, 2000) [in Russian].
3. B. I. Lazoryak and V. A. Efremov, Zh. Neorg. Khim. **32** (3), 652 (1987).
4. K. I. Petrov, M. E. Poloznikova, Kh. T. Sharipov, and V. V. Fomichev, *Vibration Spectra of Molybdates and Tungstates* (FAN, Tashkent, 1990) [in Russian].